FUDMA Journal of Sciences (FJS)
ISSN online: 2616-1370
ISSN print: 2645 - 2944
Vol. 10 No. 9, May, 2026, pp 258 – 267
DOI: https://doi.org/10.33003/fjs-2026-1009-5150

Wind Turbines Site Selection and Techno-Economic Analysis of Renewable Energy Integrated with Grid Stability Using Statistical Models

***Johnson. O. Aibangbee and Praise Iheanacho**

Department of Electrical / Electronic Engineering, Benson Idahosa University, Benin City. Edo State, Nigeria.

*Corresponding authors' email: engr.aibangbee@gmail.com Phone: +2348106493961

Received: 27 May 2026
Accepted: 24 June 2026
Published: 29 June 2026

ABSTRACT
This study analyzed the importance of wind turbines farm site selection to ensure the successful and sustainable implementation of wind energy projects. For proper site selection, factors including wind potential, topographical structure, environmental sensitivity, and legal impacts were carefully evaluated to ensure maximum performance and minimal environmental impact. Sophisticated statistical, stochastics differential equations (SDE) and economic models were utilized to optimized renewable energy integration in to the grid, develop models that predict energy output, provides grid stability, and economic impacts. By leveraging wind speed Weibull distribution and average power output data of 100 units wind turbines with 10 kW capacity each, the efficacy of these models and their potential to transform energy systems toward sustainability were demonstrated. Results showed that 95% of grid distribution stability using 70% as threshold, while 5% indicated potential instability. Energy prediction for years 2026 and 2027 ranges between 549 and 668.70 MWh with average energy of 611.754 MWh, and 614.75 MWh. The net present value **(**NPV) of the project value using discounted rate of 4-7% over 10, 15, and 20-years periods varies from $403,497,042.12 to $ 298,761,567.06; 15 years $647,373,180.32 and $468,139,101.46; and 20-years $803,031,935.24 to $562,079,265.49 respectively, depending on the discount rate. The project is considered profitable at all discount rates evaluated under the sensitivity analysis of 4 –7%, yielded a positive investment return during the whole duration of the projects, allowing for a 5% discount on infrastructure and a 7% year-on-year inflation.

Keywords: Wind Turbines, Farm Site Selection, Statistical Models, Wind Speed, Power Curve Model

INTRODUCTION

Energy is one of the most fundamental needs for sustaining life on earth according to Duranay et al, (2024), and with the rapid increase in global population, the demand for energy continues to rise. Their findings revealed that widespread use, coupled with the fact that global energy infrastructures have largely relied on them, has cemented their importance in the energy sector according to Duranay *et al*, (2024). According to American Wind Energy Association, (2014) and Olabi et *al*, (2024) in their studies proved that the use of fossil fuels has been directly linked to increasing greenhouse gas emissions, which contribute to global warming and climate change. This situation has shifted the attention of researchers to renewable energy sources, which offer a clean and inexhaustible solution to the global energy crisis.

Wind energy significantly contributes to the reduction in greenhouse gas emissions, primarily carbon dioxide, by replacing fossil fuel-based power generation. The successful operation of wind turbines is closely linked to the strategic selection of their installation sites. The success and productivity of wind energy projects are significantly influenced by factors like wind availability, terrain features, and environmental suitability. The site plays a crucial role in the efficiency of wind energy production systems by Wu, X. et al, (2020). A carefully chosen location can optimize energy production and reduce environmental impact, making the selection process crucial to the overall success of wind energy projects according to Kuczynski, et al, (2021), Bennui, *et al*, (2007) and Duranay, *et al*, (2024). Selecting a site and statistically analyzing wind speed are the most crucial factors in the development of wind farms.- Ari, and Gencer. (2020) analyzed in their studies that the typical lifespan of a wind turbine is around 20 years, and establishing wind farms involves significant costs. As a result, the process of choosing suitable locations is crucial for maximizing the return on this investment. Similarly, Embber Energy, (2024), in their studies suggested that the transition to wind energy globally is projected to play a crucial role in achieving climate targets, with estimates suggesting that wind and solar could account for over a third of the necessary emissions reductions by 2030 to limit global warming as discussed.

Modern energy modeling approach combines statistical tools are critical for improving renewable energy storage integration and guaranteeing grid security according to Benti. *et al*, (2023); Zhang, *et al*, (2014) and Owusu-Ansah *et al*, (2025). Renewable energy sources, like wind and solar power, are inherently variable and uncertain. This variability can pose significant challenges to maintaining a stable and reliable power grid as discussed by Mitra. *et al*, (2016). Correlation analysis and hypothesis testing may assist in examining the links between different renewable energy sources, grid load patterns, and possible stability problems. Monte Carlo simulations and other probabilistic modeling approaches according to Mayer, *et al*, (2023) are used to examine the effect of uncertainties related to renewable energy supply and demand changes. These simulations enable researchers to assess grid performance under a variety of scenarios, including severe weather events, and identify possible bottlenecks or weaknesses. The work by Krishnamurthy *et al*, (2024), emphasized the importance of predictive models in managing the variability of wind energy. Similarly, Kriechbaum *et al*, (2018) developed a framework

for integrating high shares of renewable energy into national energy systems. These studies underscore the need for sophisticated modeling approaches that can handle the complexities of modern energy systems. Highlighting their potential for improving the forecast accuracy of advanced statistical models Mayyahi S, *et al,* (2024). According to Bessa *et al,* (2018) and Talari, *et al,* (2018) have integrated machine learning techniques into stochastic models to demonstrate their effectiveness in simulating the uncertainty in wind power production. Their work suggests that incorporating stochastic elements into statistical modeling can significantly enhance the robustness of energy prediction. Furthermore, cost-benefit analyses of various renewable energy technologies have also been estimated by Zhao, *et al,* (2024), providing insights into their economic impacts. Their findings also suggest that while renewable energy projects often require substantial initial investments, they can offer significant long-term benefits. The location of a wind turbine has a direct impact on the efficiency, performance, and economic return of the turbine. In their studies, Duranay. *et al,* (2024), emphasized that the most basic input for wind turbines is wind speed. It is important for the wind to have a constant and continuous direction. Regular and high-speed wind areas allow for more energy production. Detailed analysis conducted to evaluate the potential of wind data which include, geographical features, assessment of environmental impacts, accessibility of infrastructure, and examination of legal conditions are among the important issues.

The study aims to examine the critical factors influencing wind turbine farm-site selection, their implications for maximizing energy production and minimize environmental disruptions as well as utilizing multifaceted techniques that incorporates statistical modeling such as autoregressive integrated moving average (ARIMA), stochastic and economic models to analyze advanced energy models that can predict energy output, integrate renewable energy into existing power grid, assess grid stability and evaluate economic viability.

MATERIALS AND METHODS

Wind Turbine Site Selection

The amount of energy that a wind farm can produce depends on the location, the size of the turbines, and the length of their blades. The site selection for wind farms is a multifaceted process, where several factors are carefully evaluated to ensure optimal performance and sustainability.

Evaluation of Wind Data

The assessment of wind data is critical to the success of a wind turbine project. These data are utilized to determine the wind potential and variability of a specific region. In a potential site for a wind turbine project, a wind measurement system should be established to measure and record wind speed. For this, anemometers are installed at various heights to collect data on wind speed. Concurrently, wind vanes are employed to ascertain the wind direction, which is crucial for the orientation and placement of the turbine. The anemometers and wind vanes are positioned at heights close to the planned rotor height of the turbine (e.g., 15 m, 30 m, 50 m). Analyzing the obtained data include the average wind speed, speed and direction distribution, and turbulence intensity, a more accurate evaluation of the temporal variations in wind speed and direction can be achieved. Consequently, this facilitates the selection of the most suitable turbines, ensuring that the installation and alignment processes are carried out with optimal efficiency.

Geographical Features and Environmental Impacts.

Geographical features hold significant importance in the site selection process for wind turbines, as they directly affect the efficiency, structural durability, and economic sustainability of the turbines. In considering the influence of wind flow, variations in wind speed and direction, turbulence effects, grid infrastructure and accessibility, restrictions on building near protected ecological sites, residential areas airports, legal factors, or in protected forest areas. It becomes evident that geographical characteristics are a critical factor in planning wind energy projects and the placement of turbines. Figure 1 depicts the factors influencing the choice of a wind turbine location. Analyzing these features ensure that wind turbines operate at maximum efficiency and have a prolonged lifespan

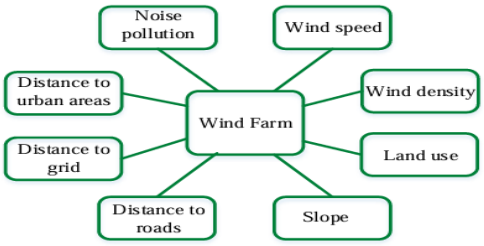

Figure 1: Factors Affecting Wind Farm Site Selection. (Source: Duranay *et, at,* 2026)

Proposed Farm Site

The proposed farm site selected for this study is Moriki village in Zurmi local government area of Zamfara state, northwestern part of Nigeria. It is located at latitude 12°52' N and longitude 6°29' E as presented in Figure 2. The availability of abundant wind energy in the village influenced the choice of wind turbines (WT) power supply in the area. The village is characterized with abundant solar and wind energy sources that can be harnessed for rural electrification. The wind speed data of Moriki village was obtained from the national aeronautics and space administration (NASA) website via HOMER software. The wind data were recorded at 10 m and 50 m respectively. The average wind speed of Moriki village at 10m is 4.49 m/s and 7.27 m/s at 50m. The wind speed rises between 3.42 m/s to 4.94 m/s at 10m, with the least wind speed recorded during the month of September and the highest recorded during the month of January. Similarly, at 50m height, the wind speed recorded ranges between 4.79 m/s to 7.41 m/s recording the least in the month of September and the highest in the month of January.

Figure 2: Map Showing the Study Location. Source: Sani Salisu *et al*, (2019)

The energy available in a wind stream is proportional to the cube of its speed, which means that doubling the wind speed increases the available energy by a factor of eight. Furthermore, the wind resource itself is seldom a steady, consistent flow. It varies with the time of day, season, height above ground, and type of terrain Nasser *et al*, (2020). At a turbine height of 30m, a cut-in wind speed of 2.5m/s was chosen for this design with the cut-out wind speed of 25 m/s; and at the rated maximum wind speed of 60m/s.

Table 1 presents the Bergey excel 10-R model wind turbine equipped with permanent magnet synchronous generator (WT-PMSG) technical specifications each rated power of 10 kW at 12 m/s is considered in this study. The 100 units wind turbines of 10 kW capacity each, are expected to operate simultaneously under the designed conditions and perform to full capacity.

Table 1: Wind Turbine with Permanent Magnet Synchronous Generator (PMSG) Specification

S/No	Item	Specification
1	Manufacturer	Bergey excel 10-R
2	Nominal Power	10 kW at 12 m/s
3	Cut-in Wind Speed	2.5 m/s
4	Cut-out Wind Speed	25 m/s
5	Max. Design Wind Speed	60 m/s
6	Furling Wind Speed	14-20 m/s
7	Drive	Direct drive
8	Generator	PMSG
9	Rated output voltage	415 V
10	Type	3 Blade Upward
11	Hub height	30 m
12	Lifespan	20 years

(Source: The Excel (2020)

The model considers 100 turbines, each rated at10 kW and generates a total of1000 kW power.
Therefore, from equation (1), P_{eq} = n× P_{kM}
Hence, equivalent power becomes P_{eq} = 100 ×10kW =1000 kW or 1.0 MW (1)
where n is the total number of wind turbines, P_{kM} is the rated power in kilowatts, and P_{eq} is the equivalent power in kilowatts.

Statistical Models
Statistical models are used to predict energy output from renewable sources. In this study, we employ time series analysis techniques such as autoregressive integrated moving average (ARIMA) and generalized autoregressive conditional heteroskedasticity (GARCH) to model the variability and predict future energy outputs.

Autoregressive Integrated Moving Average (ARIMA)
The autoregressive process of order p or AR(p) is defined as in equation (2):

$$y_t = \emptyset_1 y_{t-1} + \emptyset_2 y_{t-2} + \ldots + \emptyset_P y_{t-p} + \epsilon_t \quad (2)$$

$$y_t = \sum_{i=1}^{N} \emptyset_i y_{t-i} + \epsilon_t \quad (3)$$

where y_t is the value of the time series at time t; $\emptyset_i$ are the parameters of the model; ϵ_t is the white noise, and $\epsilon_t \sim N(0, \sigma^2)$
The $\emptyset = (\emptyset_1, \emptyset_2, \ldots, \emptyset_p)$ is the vector of model coefficients, and p is a non-negative integer. Additionally, the lag operator denoted by B is used to express lagged values of the process, so $BX_t = X_{t-1}$, $B^2 y_t = y_{t-2}$, and $B^3 y_t = y_{t-3,\ldots} B^d y_t = y_{t-1}$. The AR (p) process is given in equation (4)

$$\emptyset(B) y_t = \epsilon, \; t = 1, \ldots, n \quad (4)$$

Therefore, the moving average process of order q or MA(q) is defined as in (5):

$$y_t = \varepsilon_t + \theta_1 \varepsilon_{t-1} + \theta_2 \varepsilon_{t-2} + \ldots + \theta_q \varepsilon_{t-q} \quad (5)$$

$$y_t = \varepsilon_t \sum_{j=1}^{\varphi} \theta_j \varepsilon_{t-j} \quad (6)$$

Where, ε_t is the white noise; and θ_i are the parameters of the model.
Combining equations (2) and (6), the autoregressive moving average (ARMA) process of orders p and q can be defined as shown in equation (8),
The ARMA model of order p, q (i.e., ARMA (p, q)) combines the AR(p) and MA(q) models and can be written as follows:

$$y_t = \emptyset_1 y_{t-1} + \emptyset_2 y_{t-2} + \ldots + \emptyset_p y_{t-p} + \varepsilon_t + \theta_1 \varepsilon_{t-1} + \theta_2 \varepsilon_{t-2} + \cdots + \theta_q \varepsilon_{t-q} \quad (7)$$

$y_t = \sum_{i=1}^{p} \emptyset_1 y_{t-i} + \sum_{j=1}^{q} \theta_j \varepsilon_{t-j} + \varepsilon_t$ (8)

The ARIMA model extends the ARMA model to include differencing, which makes the time series stationary. The ARIMA model of order p, d, q can be written by applying the differencing shown in equation (8). Therefore, when we apply differencing d times to the original time series y_t to make it stationary, let z_t be the differenced series:

$z_t = (1-\mathrm{B})^d\, y_t$ (9)

where B is the backshift operator such that $By_t = y_{t-1}$.

Hence, applying the ARMA model to the differenced series z_t as shown in equation (9) leading to equation (10):

$z_t = \emptyset_1 z_{t-1} + \emptyset_2 z_{t-2} + \ldots + \emptyset_p z_{t-p} + \varepsilon_t + \theta_1 \varepsilon_{t-1} + \theta_2 \varepsilon_{t-2} + \cdots + \theta_q \varepsilon_{t-q}$ (10)

Combining equations (8) and (9) leads to equation (10);

$(1-B)^d y_t = \emptyset_1 (1-B)^d y_{t-1} + \emptyset_2 (1-B)^d y_{t-2} + \ldots + \emptyset_p (1-B)^d y_{t-p} + \varepsilon_t + \theta_1 \varepsilon_{t-1} + \theta_2 \varepsilon_{t-2} \ldots + \theta_q \varepsilon_{t-q}$ (11)

Finally, the ARIMA model can be written as follows:

$\emptyset(\mathrm{B})(1\text{-}\mathrm{B})^d y_t = \theta(\mathrm{B})\epsilon_t$ (12)

where $\emptyset(\mathrm{B}) = 1 - \emptyset_1\mathrm{B} - \emptyset_2 B^2 - \ldots - \emptyset_p B^p$ is the AR polynomial; and $\theta(\mathrm{B}) = 1 + \theta_1\mathrm{B} + \theta_2 B^2 + \ldots + \emptyset_q B^q$ is the MA polynomial.

General Autoregressive Conditional Heteroskedasticity (GARCH) Model

The GARCH model generalizes the ARCH model by including lagged values of the conditional variance Bollerslev (1986). A GARCH model of order p, q (GARCH (p, q)) can be written as (13)

$y_t = \sigma_t^2 \epsilon_t$ (13)

where y_t, σ_t^2, and ϵ_t are the return at time t.; the conditional variance of y_t; and the white noise with mean zero and variance one respectively. The conditional variance σ_t^2 is modeled as in (14),

$\sigma_t^2 = \alpha_0 + \sum_{i=1}^{q} \alpha_i y_{t-i}^2 + \sum_{j=1}^{p} \beta_j \sigma_{t-j}^2$ (14)

where $\alpha_0 > 0$; $\alpha_i \geq 0$ for i = 1, ..., q.; and $\beta_j \geq 0$ for j = 1, ..., p.

The GARCH (p, q) model includes both autoregressive (AR) terms and moving average (MA) terms for the conditional variance, capturing the persistence of volatility over time. In general, the conditional variance σ_t^2 can be expressed as an infinite sum of past squared returns (ARCH terms) and past variances (GARCH terms), providing a flexible framework for modeling volatility clustering in the data.

Stochastic Models

The study utilized stochastic models to simulate the random variability in renewable energy production. Monte Carlo simulations are used to generate a range of possible scenarios for energy production and grid stability based on the historical performance of the proposed wind farms. It is also used to model the random variability of energy output.

Grid Stability Modeling

Considering the stochastic differential equation (SDE), equation (15),

$dX_t = \mu(X_t,\mathrm{t})\,\mathrm{dt} + \sigma(X_t,\mathrm{t})\,\mathrm{d}W_t$ (15)

where X_t, $\mu(X_t,\mathrm{t})$, $\sigma(X_t,\mathrm{t})$ and W_t are the stochastic process, the drift term, the diffusion term and a wiener process or Brownian motion respectively.

Equation 16 describe the dynamics of the process X_t with two components the drift term $\mu(X_t,\mathrm{t})$ dt and diffusion term $\sigma(X_t,\mathrm{t})$ $\mathrm{d}W_t$

The term $\mathrm{d}W_t$ represents an infinitesimal increment of a wiener process W_t which has the following properties:

$\mathbb{E}[\mathrm{dW_t}] = 0$

$\mathbb{E}[(\mathrm{dW_t})^2] = \mathrm{dt}$

To find the possible solution to the stochastic differential equation, one can use the method of Itô's calculus. Assume X_t follows the SDE shown in the following equation:

$\mathrm{d}X_t = \mu\,(X_t\,\mathrm{t})\,\mathrm{dt} + \sigma\,(X_t,\mathrm{t})\,\mathrm{d}W_t$ (16)

For these solutions, the common approach is to use Itô's lemma, which provides a way to find the differential of a function of a stochastic process, let $f(X_t\ \mathrm{t})$ be a twice differentiable function. Then Itô's lemma states:

$\mathrm{df}(X_t,t) = \left(\frac{\partial f}{\partial t} + \mu(X_t,t)\frac{\partial f}{\partial X_t} + \frac{1}{2}\sigma^2(X_t,t)\frac{\partial^2 f}{\partial X_t^2}\right)dt + \sigma(X_t,t)\frac{\partial f}{\partial X_t}dW_t$ (17)

Considering the Geometric Brownian Motion (GBM), where $\mu\ (X_t,\mathrm{t}) = \mu X_t$, and $\sigma\ (X_t,\mathrm{t}) = \sigma X_t$ the SDE and GBM is as follows:

$dX_t = \mu X_t dt \quad + \sigma X_t \mathrm{d}\, W_t$ (18)

To solve this SDE, we use the method of separation of variables and Itô's lemma. Define $Y_t = \mathrm{In}\ (X_t)$. Applying Itô's lemma to $Y_t = \mathrm{In}\ (X_t)$:

$dY_t = \frac{\partial \mathrm{In}(\mathrm{X_t})}{\partial X_t}\mathrm{d}X_t + \frac{1}{2}\frac{\partial^2 \mathrm{In}(\mathrm{X_t})}{\partial \mathrm{X_t}^2}(\mathrm{d}X_t)^2$ (19a)

$= \frac{1}{X_t}(\mu X_t\,\mathrm{dt} + \sigma\, X_t\, dw_t) - \frac{1}{2}\frac{1}{\mathrm{X_t}^2}(\sigma X_t)^2\,\mathrm{dt}$ (19b)

$= \mu\mathrm{dt} + \sigma\,\mathrm{d}W_t \ - \frac{1}{2}\sigma^2\,\mathrm{dt}$ (19c)

$= (\mu - \frac{1}{2}\sigma^2)\,\mathrm{dt} + \sigma\,\mathrm{d}W_t$ (19d)

Integrating both sides, we have:

$Y_t = Y_0 + (\mu - \frac{1}{2}\sigma^2)\,\mathrm{t} + \sigma W_t$ (20)

Since $Y_t = \mathrm{In}\ (X_t)$, exponentiating both sides yields:

$X_t = \mathrm{X}_0 \exp((\mu - \frac{1}{2}\sigma^2)\,\mathrm{t} + \sigma W_t)$ (21)

Hence, the solution to the SDE for Geometric Brownian Motion, with the process X_t, evolves over time.

Economic Models

This study incorporates economic models to evaluate financial implications of different energy integration strategies. Optimization techniques and cost-benefit analysis are employed to determine the most economically viable alternatives for integrating renewable energy. In order to determine the value of a series of cash flows. The NPV is calculated by discounting future cash flows back to their present value using a discount rate. Considering a single cash flow, the present value (PV) of a single cash flow C_t occurring at time t is calculated as in (22),

$\mathrm{PV_t} = \frac{C_t}{(1+\mathrm{r})^{\mathrm{t}}}$ (22)

Where $(1+r)^t$ is the discount factor that accounts for the time value of money, discounting the future cash flow C_t back to the present time.

The NPV is the sum of the present values of all individual cash flows from time 0 to time n as shown in (30):

$\mathrm{NPV} = \sum_{t=0}^{n} \mathrm{PV_t} = \sum_{t=0}^{n} \frac{C_t}{(1+r)^t}$ (23)

Incorporating the initial investment C_0 and all subsequent cash flow C_1, C_2, …., C_n, the following is obtained:

$\mathrm{NPV} = \frac{C_0}{(1+r)^0} + \frac{C_1}{(1+r)^1} + \frac{C_2}{(1+r)^2} + \ldots. + \frac{C_n}{(1+r)^n}$ (24)

$= c_0 + \frac{\boldsymbol{c_1}}{\mathbf{1+r}} + \frac{\boldsymbol{c_2}}{\mathbf{(1+r)^2}} + \mathbf{\ldots.} + \frac{C_n}{(1+r)^n}$ (24a)

Therefore, the NPV formula effectively discounts each future cash flow back to its present value and suns them up, providing the total NPV of the cash flows.

Hence, incorporating the revenue at time t, the NPV is calculated as in (25);

$\mathrm{NPV} = \sum_{t=0}^{T} \frac{R_t - C_t}{(1+r)^t}$ (25)

where: C_0, C_t, R_t, and r are the initial investment (usually a negative value representing an outflow), the cost at time t., the revenue at time t, and the discount rate respectively.

Wind Turbine Power Curve

Wind speed is the primary factor influencing turbine power generation. The power output of a turbine is proportional to the cube of the wind speed, meaning small changes in speed can lead to substantial differences in energy production according to Duranay *et al*, (2024). In the conversion of wind speed data into energy output, the turbine power curve plays a crucial role in achieving the total power output. The power curve of a wind turbine describes the relationship between the wind speed and the electrical power output of the turbine according to Duranay *et al*, (2024). The power P generated by a wind turbine can be expressed as a function of wind speed v, air density ρ, rotor swept area A, and power coefficient C_p. The kinetic energy in the wind per unit time passing through an area A is given by:

$$P_{wind} = \frac{1}{2}\rho A C_p v^3 \quad (26)$$

Where, ρ is the air density (kg/m³); A is the rotor swept area (m²); and *V* is the wind speed (m/s).

The power coefficient C_p represents the efficiency with which the wind turbine converts the kinetic energy in the wind into mechanical energy according to DeLellis, *et al*, (2018). It is a dimensionless number that varies with wind speed and the design of the turbine. The maximum value of C_p is given by Betz's limit, which is approximately 0.59. Therefore, actual power output P of the wind turbine is given as in (27):

$$P = \frac{1}{2}\rho A C_p v^3 \quad (27)$$

Each turbine has its own characteristics. In order to accurately calculate the output of a particular turbine at a specific wind speed, it is required to use its power curve. Figure 3 shows the power–speed characteristics of Northern Power Systems (NPS) wind turbine according to Duranay, *et al*, (2024). The power–speed characteristic of a wind turbine power curve describes show the output power changes with wind speed. This curve is generally divided into four key regions as shown in Figure 3.

i. Region 1 (cut-in wind speed): The minimum wind speed at which the turbine starts to generate power. Below this speed, power output is zero. The cut-in wind speed in Figure 4 is 3m/s. In this region, the turbine starts generating power at the cut-in wind speed v_{cut-in}. The power output increases with the cube of the wind speed up to the rated wind speed v_{rated}

$$P = \begin{cases} 0 & if\ v < v_{cut-in} \\ \frac{1}{2}\rho A C_p v^3 & if\ v_{cut-in} \le v \le v_{rated} \end{cases} \quad (28)$$

ii. Region 2 (rising power): between the cut-in speed and the rated speed, the power output increases with the cube of the wind speed, following the equation mentioned above.

iii. Region 3 (rated power): When the wind speed reaches the rated speed, the turbine operates at its maximum rated power. This region represents a constant power output, achieved by adjusting the blade pitch or using control systems to avoid overloading. In this region, the power output is constant and equals the rated power P_{rated}:

$$P = \{P_{rated} \quad \text{if } v_{rated} < v \le v_{cut\text{-}out} \quad (29)$$

iv. Region 4 (cut-out wind speed): If the wind speed exceeds a certain limit (the cut-out speed), the turbine is shut down to prevent mechanical damage, and the power output drops to zero.

$$P = \{0 \quad \text{if } v > v_{cut\text{-}out} \quad (30)$$

The cut-out wind speed in Figure 1 is 25m/s.

Combining all the regions comprising of equations (28) – (30), the complete power curve equation can be written as follows:

$$P = \begin{cases} 0 & if\ v < v_{cut-in} \\ \frac{1}{2}\rho A C_p v^3 & if\ v_{cut-in} \le v \le v_{rated} \\ P_{rated} & if\ v_{rated} < v \le v_{cut-out} \\ 0 & if\ v > v_{cut-out} \end{cases} \quad (31)$$

where, v_{cut-in} is the Cut-in wind speed where the turbine starts to generate power; v_{rated} is the rated wind speed where the turbine reaches its rated power output; $v_{cut-out}$ is the cut-out wind speed where the turbine stops to avoid damage; ρ: = Air density, typically around 1.225 kg/m³ at sea level; A = rotor swept area, A = πR^2, where R is the rotor radius; and C_p = power coefficient, typically less than or equal to 0.593.

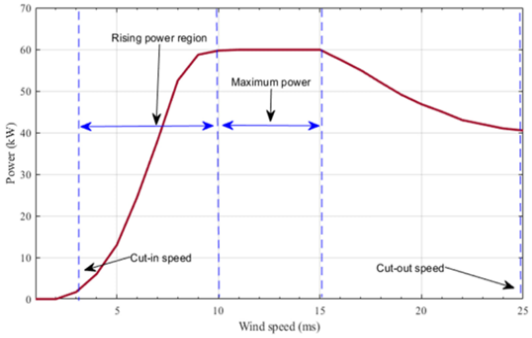

Figure 3. Power–Speed Curve of Wind Turbine (Source: Duranay, *et al*, 2026)

The study uses data of the wind farm with 100 turbines, each with a capacity of 10 kW. Wind speed data were used to simulate 10 years of hourly wind speed. The wind speed follows Weibull distribution which is represented as in (32);

$$f(x;\lambda,k) = \frac{k}{\lambda}\left(\frac{x}{\lambda}\right)^{k-1} * e^{-(x/\lambda)^k} \quad \text{for } x \ge 0 \quad (32)$$

Where $\lambda > 0$ is the scale parameter; $k > 0$ is the shape parameter; and x is the random variable. Hence, the cumulative distribution function of the Weibull distribution is given as:

$$F(x;\lambda,k) = \begin{cases} 1 - e^{-(\frac{x}{\lambda})^k} & for\ x \ge 0 \\ 0 & for\ x < 0 \end{cases} \quad (33)$$

Wind turbines offer significant advantages as a clean, renewable, and cost-effective energy source, producing no emissions while utilizing free wind to generate electricity.

RESULTS AND DISCUSSION

Farms site selection for wind turbines is a multifaceted process, where several factors were carefully evaluated to ensure optimal performance and sustainability. Based on

research findings on site selection for wind turbine farms factors such as potential of wind data, geographical features, social impacts, assessment of environmental impacts, accessibility of infrastructure, and legal conditions were among the important factors influencing the selection of wind turbines farms site. This research contributes significantly to the development of effective energy projects that align with sustainability and efficiency of wind energy systems. The relationship between these factors is integral to the successful implementation of wind energy projects, which ensure they operate at maximum efficiency and minimize ecological disruption.

Power Turbine Curve

Employing the power turbine curve equations, the power curve for the wind turbine, given the parameters for the Weibull distribution for the wind speed, as defined in equation (34). The power curve equation for a wind turbine, is substituted with the given parameters as in (34),

$$P(V) = \begin{cases} 0 & if\ v < 3ms^{-1} \\ 10\left(\frac{v-3}{9}\right)^3 & if\ 3ms^{-1} \leq v < 12ms^{-1} \\ 10 & if\ 12ms^{-1} \leq v < 25ms^{-1} \\ 0 & if\ v > 25ms^{-1} \end{cases} \quad (34)$$

where P(v) is the power output at wind speed v; 3 ms^{-1} is the cut-in wind speed; 12 ms^{-1} is the rated wind speed; 25 ms^{-1} is the cut-out wind speed; and 10 kW is the rated power of each turbine.

This result shows the piece-wise continuous function within the domains for which the power output functions. The essential inputs include a 3m/s cut-in wind speed, a 12m/s rated wind speed, a 25m/s cut-out speed, and 100 units turbines-PMSG of 10 kW capacity each, totally 1000 kW rated power of the turbines. These domains are critical for the smooth functioning of the turbines data. Based on these, the projected average power output for each year over a 10-year period is presented in Table 2.

Table 2: Projected 10 Year Average Power Output Measured in Megawatt Hour (MWh)

Month Year	Jan.	Feb.	March	April	May	June	July	Aug.	Sept	Oct.	Nov.	Dec.
1	553.25	553.9	554.0	553.1	553.25	553.15	552.65	552.55	552.90	553.00	553.45	553.95
2	553.65	553.75	553.45	553.75	553.95	553.55	553.6	553.65	553.00	553.05	552.85	553.85
3	553.20	553.6	553.60	553.40	553.25	552.85	553.10	553.30	553.50	553.75	553.45	553.20
4	553.55	553.25	553.70	553.65	553.05	553.10	553.70	553.40	553.65	553.45	553.85	553.65
5	553.15	553.40	553.30	553.50	553.80	553.30	553.40	553.15	553.25	553.15	553.30	553.45
6	553.40	553.50	553.70	553.50	553.40	553.60	553.10	553.50	553.15	553.00	553.60	553.60
7	553.35	553.35	553.40	553.40	553.50	553.15	553.20	553.55	553.50	553.30	553.35	553.40
8	553.40	553.55	553.55	553.55	553.45	553.30	553.45	553.30	553.55	553.55	553.70	553.45
9	553.60	553.40	553.50	553.60	553.70	553.45	553.45	553.50	553.60	553.75	553.45	553.60
10	553.60	553.30	553.40	553.70	553.45	553.60	553.40	553.55	553.70	553.45	553.30	553.40

As indicated in Table 2, the power output remains consistent within the range of 553 -553.95 MW to monthly average power output for each year over the 10-year period. The consistency range of power output is as a result of the modeling procedure itself as it varies slightly and thus makes room for dynamism and changes in the wind speed to provide for the consistent power output. Figure 4 presents the wind speed variations during the twelve months of the year. The wind speed indicates that Moriki village has the require wind speed for wind power generation.

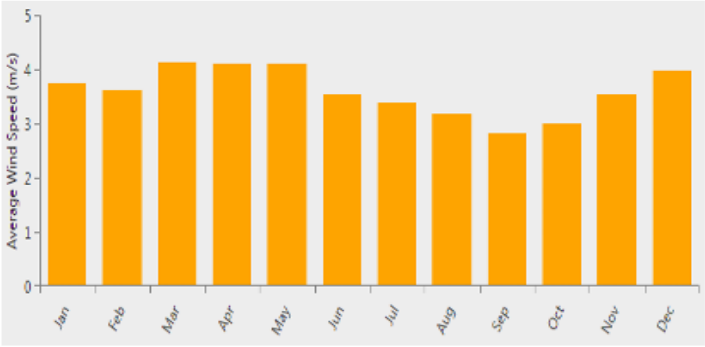

Figure 4. Average Wind Speed Variation During the Year

Autoregressive Integrated Moving Average model

Based on the autocorrelation function (ACF) and partial autocorrelation function (PACF) graphs, the ARIMA model's fitting and forecasting procedure determined that the ARIMA (1,1,1) model was appropriate. The loss of information criteria used for the ARIMA model was found to be 429.265 for Akaike Information Criteria and 438.796 for Bayesian Information Criteria, though the HQIC had another less figure, thus triangulating these two results and showing a lower loss of information and the appropriateness of ARIMA (1,1,1). While analyzing the ACF and the PACF, the cutoff occurs after the first lag on each plot, deepening the choice of ARIMA (1,1,1) as it's justified by theories of time series in Figure 5, and Table 3 respectively.

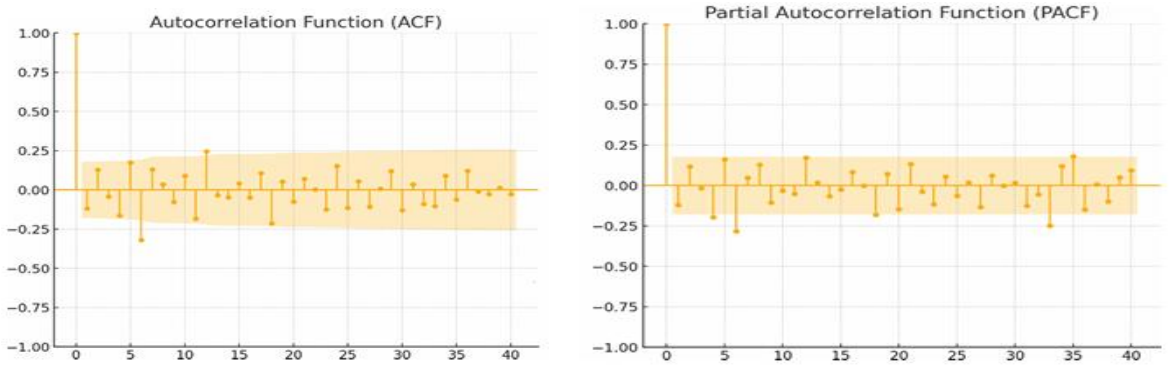

(a) (b)

Figure 5: (a) Autocorrelation Function and (b) Partial Autocorrelation Function Plots

Table 3: Autoregressive Integrated Moving Average Model Results

Statistic	Value
Dependent variable	D.y
Number of observations	119
Model	ARIMA (1,1,1)
Loglikelihood	−211.531
Method	CSS-MLE
Standard Deviation of innovations	0.083
Akaike Information Criterion (AIC)	429.265
Bayesian Information Criterion (BIC)	438.796
Hannan–Quinn Information Criterion (HQIC)	433.091

Additionally, the residuals were tested for white noise using the Ljung-Box test. It is evident in the use of the residual plots that the residuals pass the test, which confirms that the model is appropriate. It shows that the residuals are normally distributed, indicating that the model fits the data well as shown in Figure 6 (a) and (b). while Table 4 presents the coefficient of the ARIMA model needed for the forecasting.

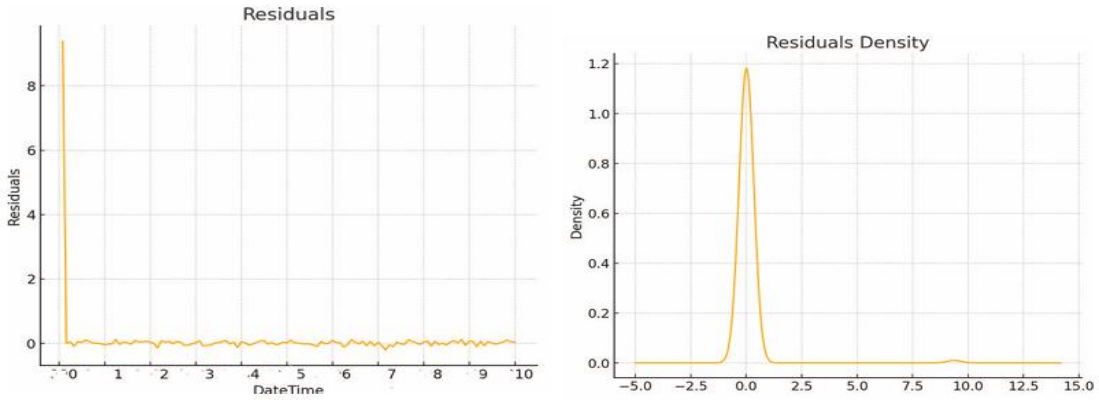

(a) (b)

Figure 6: (a) Residuals and (b) Residual Density Plots

Table 4. Coefficients of the Autoregressive Integrated Moving Average Model

Term	Coefficient	Std. error	z-Statistic	P-value
Const	0.0031	0.001	2.470	0.014
AR.L1.D.y	-0.0868	0.092	-0.928	0.352
MA.L1.D.y	0.0003	0.091	0.003	0.997

Forecasting

By using the ARIMA model that has been adjusted to the data, we are able to make a forecast of the energy production for the next year. The monthly energy output for the next two years 2026 and 2027 is shown in Table 5. The projected average energy for the next year is 611.754, with a standard deviation of 29.055. In the following year, the average energy is expected to be 614.75, with a deviation of 8.353. The second year had a steady energy production, which may have contributed to the smooth operations after the first setup. Furthermore, there was a steady prediction of electricity generation for the next two years, consistently ranging between 549 and 668.70 megawatts-hours.

Table 5: Monthly Power Output in Megawatts Hour for the Year 2026 and 2027

Months	Two Years Monthly Forecasted Power Output (MWh)	
	2026	**2027**
January	594.15	599.10
February	598.45	601.9
March	624.35	627.10
April	549.75	552.75
May	629.00	632.40
June	611.75	614.55
July	665.55	668.70
August	642.60	645.70
September	612.30	614.35
October	619.45	621.55
November	606.40	608.40
December	587.45	559.03
Average	611.754	614.75
Standard deviation	29.055	8.353

Grid Stability Analysis Using the Monte Carlo Simulation

The Monte Carlo simulation was performed to assess grid stability under varying energy output scenarios. For this, multiple scenarios of energy output were generated using the predicted mean and standard deviation from the ARIMA model. A simulation is run to assess the grid stability for each scenario. Using the SDE for grid stability, we simulate the state variable X_t for 10,000 iterations, each representing a different possible future scenario.

The SDE used for simulation is shown with time steps of 252, and thus one year of daily simulations and results are presented in Figure 7. Results showed that 95% of scenarios resulted in grid stability within acceptable limits, thus using 70% as threshold, while 5% indicated potential instability, which would require intervention measures such as energy storage or demand response. The distribution of grid stability outcomes is presented in Figure 7. Majority of the scenarios under consideration were having stability from 70% to 97%, indicating a better coverage of power output with less instability that needed to be catered for. However, scenario 61 saw the least stability analysis to outcome followed by scenarios 20, 38, and 91 which all performed less than the threshold of 70% as indicated in Figure 7:

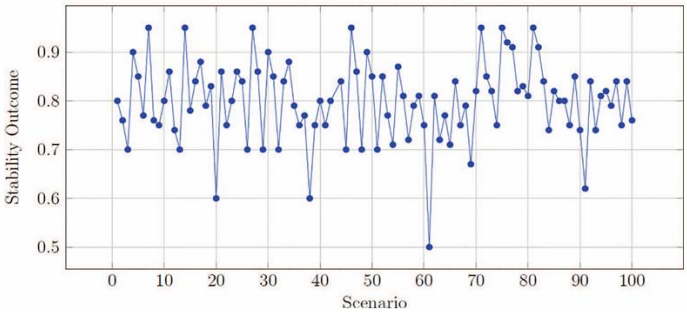

Figure 7: Monte Carlo Simulations of Grid Distribution Stability

Economic Impact Evaluation

In order to maintain interest and attract capital investment, this research conducted an NPV analysis to assess the financial feasibility of integrating the wind farm into the grid. This assessment is based on the calculation of the yearly income and expenses, taking into account the projected energy production and market price of energy output. Based on the average monthly power output, using a take or pay cost pricing model at a rate of $0.10 per kilowatt-hour (kWh) from the bulk power producers' base rate, and considering a 5% loss in revenue due to inefficiency and late payment settlement, the actual monthly cash flow revenue estimation amounts to $10,508,477.50. Taking into consideration an uncertainty of ± $ 2 million per month. The yearly income amounts to about $126,100,730 each year, as depicted in Table 6.

Table 6: Revenue Generation and Computation of Net Present Value

Parameter	Amount
Effective monthly revenue at 5% loss	$10,508,477
Annual revenue	$126,100,730
Initial investment cost	$ 400 million
Discount	5%
Maintenance, tax, and remuneration	$20 million
Inflation on maintenance, tax and remuneration	7% per annum
Price per kilowatts rate	$0.10
Project life time	20 years

With an initial investment of $400 million, discounted at 5%, with maintenance, tax, and remuneration at $20 million per annum with a year-on-year inflation of 7%, and finally a project life time of 20 years, the NPV is estimated for 10, 15, and 20 years to quantify the profitability and worthiness of investing in this infrastructure.

Net Present Value and Sensitivity Analysis

The NPV of the projected value, discounted at a rate of 5%, yielded a positive return during the whole duration of the projects. The amount over a period of 10 years was $366,054,677.13, for a period of 15 years amounted to $581,739,184.58, and for a period of 20 years it was $713,048,178.22. The sensitivity analysis involves altering the discount rate within the range of 4–7%. The NPV findings for each time period are shown in Table 7. The NPV of the project over a 10-year period varies from $403,497,042.12 to $ 298,761,567.06. Over the course of 15 years, the NPV varies between $647,373,180.32 and $ 468,139,101.46. Similarly, in the 20-year project, the NPV ranges from $803,031,935.24 to $562,079,265.49, depending on the discount rate. The investment is consistently lucrative throughout all examined time frames, with strong NPVs suggesting that the project is expected to return much more income than the original expenditure. Despite the increase in discount rates, the NPV remains positive, which strengthens the project's resilience to fluctuations in discount rates. As the investment time increases, the NPV also increases. A project's profitability is maximized when it spans a duration of 20 years. The study has taken into account the 7% inflation rate for yearly expenses, and the NPVs continue to be advantageous.

Table 7: Sensitivity Analysis on Net Present Value

Discount Rate (%)	10 Years ($)	15 Years ($)	20 Years ($)
4	403,497,042.12	647,373,180.32	803,031,935.24
5	366,054,677.13	581,739,184.58	713,048,178.22
6	331,216,891.41	522,224,968.03	633, 191,555.80
7	298,761,567.06	468,139,101.46	562,079,265.49

CONCLUSION

This study analyzed the importance of farm site selection in wind energy projects, emphasized factors impacting on project efficiency, sustainability, and environmental compatibility. Factors such as wind potential, topographical features, environmental sensitivities, community interactions, legal permits, and available infrastructure were critically evaluated to optimize the performance of wind turbines. Selecting appropriate locations for wind turbines farm, can enhance energy production, foster community support, and ensure compliance with environmental standards. The study also evaluated the use of the wind distribution modeled from the Weibull distribution, along with a wind farm comprising 100 turbines-PMSG of 10 kW capacity each using advanced statistical modeling tools such as ARIMA, and stochastic differential equation (SDE) to build a comprehensive energy modeling with a grid stability analysis; that with the required wind speed domains can create an average electricity production of approximately 614 MWh every month. Optimization algorithms were employed to determine integrating renewable energy sources into the power system, while economic analyses were conducted to evaluate the financial viability of renewable energy project with various discount rates and project lifetimes. Estimating the cost of KWh at $0.10 market rate, the project is considered profitable at all discount rates evaluated under the sensitivity analysis of 4 –7%, allowing for a 5% discount on infrastructure and a 7% year-on-year inflation.

Conflicts of Interest

The authors declare no conflicts of interest.

REFERENCES

Al-mayyahi S, Yahya K, Yahya AEM, Sarreb RD, Ald ababsa M. Machine learning techniques for solar power output predicting. Int J Smart Grid. 2024;8(2):98–107. doi: https://doi.org/10.20508/ijsmartgrid. v8i2341.g356

American Wind Energy Association. The Clean Air Benefits of Wind Energy; American Wind Energy Association: Washington, DC, USA, 2014.

Ari, E.S. and Gencer, C. Proposal of a novel mixed integer linear programming model for site selection of a wind power plant based on power maximization with use of mixed type wind turbines. Energy Environ. 2020, 31, 825–841. [CrossRef]

Bennui, A.; Rattanamanee, P.; Puetpaiboon, U.; Phukpattaranont, P.; Chetpattananondh, K. Site selection for large wind turbine using GIS. In Proceedings of the PSU-UNS International Conference on Engineering and Environment, Phuket, Thailand, 10–11 May 2007

Benti NE, Chaka MD, Semie AG. Forecasting renewable energy generation with machine learning and deep learning: current advances and future prospects. Sustainability. 2023;15(9):7087. doi: https://doi.org/10.3390/su15097087

Choukulkar, A.; Pichugina, Y.; Clack, C.T.; Calhoun, R.; Banta, R.; Brewer, A.; Hardesty, M. A new formulation for rotor equivalent wind speed for wind resource assessment and wind power forecasting. Wind Energy 2016, 19, 1439–1452. [CrossRef]

DeLellis, M.; Reginatto, R.; Saraiva, R.; Trofino, A. The Betz limit applied to airborne wind energy. Renew. Energy 2018, 127, 32–40. [CrossRef]

Duranay, Z.B.; Güldemir, H.; Co¸skun, B. The Role of Wind Turbine Siting in Achieving Sustainable Energy Goals. Processes 2024, 12, 2900. Doi: https://doi.org/10.3390/pr12122900

Embber Energy. Why Wind and Solar Are Key Solutions to Combat Climate Change. Available online: https://ember-energy.org/latest-insights/why wind and solar are key solutions to combat climate change/ (accessed on 10 December 2024).

Juma, M.I.; Mwinyiwiwa, B.M.M.; Msigwa, C.J.; Mushi, A.T. Design of a Hybrid Energy System with Energy Storage

for Standalone DC Microgrid Application. Energies 2021, 14, 5994. Doi: https://doi.org/10.3390/en14185994

Kriechbaum L, Scheiber G, Kienberger T. Grid-based multi energy systems modelling, assessment, opensource mod elling frameworks and challenges. Energy Sustain Soc. 2018;8:35. doi: https://doi.org/10.1186/s13705-018-0176-x

Krishnamurthy S, Adewuyi OB, Luwaca E, Ratshitanga M, Moodley P. Artificial intelligence-based forecasting models for integrated energy system management planning: an exploration of the prospects for South Africa. Energy Convers Manag. 2024;24:100772. doi: https://doi.org/10.1016/j.ecmx.2024.100772

Kuczynski, W.; Wolniewicz, K.; Charun, H. Analysis of the wind turbine selection for the given wind conditions. Energies 2021, 14, 7740. [CrossRef]

Mamaghani A.H, Escandon, S. A. A. Najafi, B. Shirazi, A. and F. Rinaldi, F. "Techno-economic feasibility of photovoltaic, wind, diesel and hybrid electrification systems for off-grid rural electrification in Colombia," Renewable Energy, vol. 97, pp. 293-305, 2016.

Mayer MJ, Biró B, Szücs B, Aszódi A. Probabilistic modeling of future electricity systems with high renewable energy penetration using machine learning. Appl Energy. 2023;336:120801. doi: https://doi.org/10.1016/j.apenergy.2023.120801

Mitra J, Vallem MR, Singh C. Optimal deployment of dis tributed generation using a reliability criterion IEEE Trans Ind Appl. 2016;52(3):1989–97. doi: https://doi.org/10.1109/TIA.2016.2517067

Nasser Yimen, Theodore Tchotang, Abraham Kanmogne, Idriss Abdelkhalikh Idriss, Bashir Musa, Aliyu Aliyu, Eric C. Okonkwo, Sani Isah Abba, Lucien Meva'a, Oumarou Hamandjoda, and Mustafa Dagbasi. "Optimal Sizing and Techno-Economic Analysis of Hybrid Renewable Energy Systems—A Case Study of a Photovoltaic/Wind/Battery/Diesel System in Fanisau, Northern Nigeria" Processes 2020, 8, 1381

Olabi, A.G.; Obaideen, K.; Abdelkareem, M.A.; AlMallahi, M.N.; Shehata, N.; Alami, A.H.; Sayed, E.T. Wind energy contribution to the sustainable development goals: Case study on London array. Sustainability 2023, 15, 4641. [CrossRef]

Owusu-Ansah EDJ, Avuglah RK, Harris E, Kyere AY, Amankwaa BD. Optimizing renewable energy integration: statistical models for grid stability and economic viability. Academia Green Energy 2025;2. https://doi.org/10.20935/AcadEnergy7430

Ren, G.; Liu, J.; Wan, J.; Li, F.; Guo, Y.; Yu, D. The analysis of turbulence intensity based on wind speed data in onshore wind farms. Renew. Energy 2018, 123, 756–766. [CrossRef]

Sani Salisu, Mohd Wazir Mustafa, Olatunji Obalowu Mohammed, Mamunu Mustapha, Touqeer Ahmed Jumani. "Techno-Economic Feasibility Analysis of an Off-grid Hybrid Energy System for Rural Electrification in Nigeria" International Journal of Renewable Energy Research Vol.9, No.1, March, 2019.

Sultan, A.Y.; Charabi, Y.; Gastli, A.; Al-Alawi, S. Assessment of wind energy potential locations in Oman using data from existing weather stations. Renew. Sustain. Energy Rev. 2010, 14, 1428–1436.

Talari S, Shafie-khah M, Osório GJ, Aghaei J, Catalão JPS. Stochastic modelling of renewable energy sources from operators' point-of-view: a survey. Renew Sustain Energy Rev. 2018;81:1953–65. doi: https://doi.org/10.1016/j.rser.2017.06.006

The Excel 10 kW Wind Power. Available online: https://www.bergey.com/products/wind-turbines/10kw-bergey-excel (accessed on 4 September 2020).

Wind Turbine Models. Available online: https://en.wind-turbine-models.com/turbines/1270-nps-northern-power-nps-60-24 (accessed on 15 October 2024).

Wu, X.; Zhang, C.; Jiang, L.; Liao, H. An integrated method with PROMETHEE and conflict analysis for qualitative and quantitative decision-making: Case study of site selection for wind power plants. Cogn. Computing. 2020, 12, 100–114. [CrossRef]

Zhang Y, Wang J, Wang X, Zhao D. Review on probabilistic forecasting of wind power generation. Renew Sustain Energy Rev. 2014;32:255–70. doi: https://doi.org/10.1016/j.rser.2014.01.032

Zhao Y, Zeng S, Ding Y, Ma L, Wang Z, Liang A, Ren H. Cost-benefit analysis of distributed energy systems considering the monetization of indirect benefits. Sustainability. 2024;16(2):820. doi: https://doi.org/10.3390/su16020820